A boundary element solution for 2-dimensional viscous sintering

Eindhoven University of Technology
Department of Mathematics and Computing Science

RANA 90-10
October 1990

A BOUNDARY ELEMENT SOLUTION FOR 2-DIMENSIONAL VISCOUS SINTERING

by
G.A.L. van de Vorst
R.M.M. Mattheij
H.K. Kuiken

Reports on Applied and Numerical Analysis
Department of Mathematics and Computing Science
Eindhoven University of Technology
P.O. Box 513
5600 MB Eindhoven
The Netherlands

A boundary element solution for 2-dimensional viscous sintering

G.A.L. van de Vorst
R.M.M. Mattheij
H.K. Kuiken

Subject classifications: 65R99, 76D07
Keywords : sintering, viscosity, boundary element method, moving boundaries.

A boundary element solution for 2-dimensional viscous sintering

G.A.L. van de Vorst
R.M.M. Mattheij
H.K. Kuiken*

Department of Mathematics
University of Technology
P.O. Box 513, 5600 MB Eindhoven
The Netherlands.

Abstract

By viscous sintering is meant processes in which a granular compact is heated to a temperature at which the viscosity of the material under consideration becomes low enough for surface tension to cause the powder particles to deform and coalesce. For the sake of simplicity this process is modeled in a two-dimensional space. The governing (Stokes) equations describe the deformation of a two-dimensional viscous liquid region under the influence of the curvature of the outer boundary. However, some extra conditions are needed to ensure that these equations can be solved uniquely. A boundary element method is applied to solve the equations for an arbitrarily initial-shaped fluid region. The numerical problems that can arise in computing the curvature, in particular when this is varying rapidly, are discussed. A number of numerical examples are shown for simply connected regions which transform themselves into circles as time increases.

*Other address: Philips Research Laboratories, P.O. Box 80.000, 5600 JA Eindhoven. The Netherlands.

1 Introduction

When powders of metals, ionic crystals, or glasses are heated to temperatures near to their melting points, the powder particles weld together and the density of the compact changes: this process is known as sintering. Sintering is a process which reduces the total surface of the powder particles. The driving force arises from the excess free energy of the surface of the powder over that of the solid material.

There are a number of physical principles which can be held responsible for the sintering phenomena; for a review see for example Exner [4]. We are mainly interested in the case of sintering when the material transport can be modeled as a viscous Newtonian volume flow, driven solely by surface tension (viscous sintering). This gives us a simple model of what is known as the sol-gel technique, which can for example be used to produce high-quality glasses. In this technique a glassy aerogel is heated to a temperature at which the viscosity of the glass becomes low enough for surface tension acting on the interior surface of the gel to cause the gel to collapse into a dense homogeneous material.

It is impossible to give a deterministic description of the flow within such a complex sintering geometry as an aerogel. We shall therefore investigate simple geometries; to start with in 2-D only, aiming to eventually derive constitutive laws of the effects obtained.

A classical problem in sintering literature is the two-dimensional initial-stage unit model, the sintering of two cylinders, which has been solved exactly by Hopper [5,6]. The sintering of an infinite line of cylinders was simulated numerically by Ross *et al.* [16]. They were also the first to perform the simulation using a Finite Element Method (FEM). Jagota and Dawson [8,9] have recently reported some results obtained with the Finite Element Method for the sintering of two spheres and an infinite line of cylinders (i.e. 3-dimensional axisymmetric problems). Recently, Kuiken [10] applied a Boundary Element Method to solve viscous sintering problems for bodies with rather smooth boundaries. A review about the available numerical techniques for such creeping Stokes flow, has recently been given by Weinbaum [17].

In this paper we present another way of implementing a Boundary Element Method for viscous sintering problems. Our aim is to develop a code which tells us how a fluid with an arbitrarily shaped region transforms itself through time, driven only by the surface tension. To compute the shape at different time steps, we only need to know the velocity of the outer boundary points. This gives us the motivation to use a Boundary Element Method rather than a Finite Element Method. Another reason for using a BEM is the fact that remeshing a boundary curve is much easier than remeshing a full 2-dimensional grid, as is done in a Finite Element Method.

Firstly, we shall rewrite the viscous sintering problem, which is described by a set of partial differential equations, into a set of integral equations. Then we shall show analytically that the integral equations derived for an arbitrary region still

have three degrees of freedom; so three extra conditions must be given to ensure that the problem can be solved uniquely. These integral equations are solved by a BEM, as proposed by Brebbia [2]. Further, we shall discuss the numerical problems that arise in computing the curvature, in particular when this is varying rapidly. Finally, we shall give a number of numerical examples to demonstrate the usefulness of our method.

2 Problem formulation

In this paper we assume that the viscous sintering problem can be modeled by a viscous incompressible Newtonian fluid flow. This flow is characterized by the dynamic viscosity η, the surface tension γ and the magnitude of the body (characterized by its cross-section, e.g. length ℓ). We denote the *velocity* of the fluid with $\mathbf{v}$ and the *pressure* with p. The region of flow is defined by a closed curve Γ and the interior area denoted by Ω.
For a viscous sintering problem the creeping flow Stokes equations hold (Kuiken [10]):

$$\begin{aligned} \eta \triangle \mathbf{v} - \text{grad p} &= 0 \\ \text{div } \mathbf{v} &= 0. \end{aligned} \tag{2.1}$$

We define a *characteristic velocity* v_c, a *characteristic pressure* p_c and a *characteristic time* τ by:

$$v_c = \gamma/\eta, \qquad p_c = \gamma/\ell, \qquad \tau = \ell\eta/\gamma. \tag{2.2}$$

We use these characteristic parameters to obtain a dimensionless formulation for (2.1)

$$\begin{aligned} \triangle\tilde{\mathbf{v}} - \text{grad } \tilde{\text{p}} &= 0 \\ \text{div } \tilde{\mathbf{v}} &= 0. \end{aligned} \tag{2.3}$$

We shall omit the dash $\tilde{}$ further on when we mean the dimensionless velocity ($\mathbf{v}$) or the dimensionless pressure (p).
On the boundary the normal component of the stress vector is proportional to the local curvature κ of Γ. This condition can be expressed as:

$$\mathcal{T}\mathbf{n} = (\text{div } \mathbf{n})\mathbf{n} \tag{2.4}$$

where $\mathbf{n}$ is the outward unit normal vector of Γ and $\mathcal{T}$ is the stress tensor.
The model described above does not ensure a unique solution. A superimposition of an arbitrary rigid-body translation or an arbitrary rigid-body rotation upon any particular solution will not alter the stress field at the boundary Γ. Thus we need to add three extra conditions to ensure that the velocity field obtained is unique. These conditions will be derived in section 3.1.

If we were to solve the problem defined above for a fixed boundary Γ we would find, in general, a non-zero flow field on Γ; this would mean an inflow through one part of the boundary and an outflow elsewhere; this is unphysical because Γ is a material boundary. Hence Γ is moving; its displacement can be found from the velocity field just derived

$$\frac{d\mathbf{x}}{d\tau} = \mathbf{v}(\mathbf{x}), \qquad (\mathbf{x} \in \Gamma) \tag{2.5}$$

subject to an initial boundary Γ_0 at $\tau = \tau_0$.
We note that the driving force of this problem is the curvature κ (=div n) along the boundary curve Γ. When the curvature is constant along Γ, i.e. when Γ is a circle, the normal component of the stress tensor is constant. Since we assume no arbitrary rigid-body translation or rotation, the velocity field of the boundary Γ will be equal to zero. Thus our initial boundary Γ_0 will be transformed into a circle when $\tau \to \infty$ (physically: the minimal surface energy of the body).

3 Boundary Integral Formulation

We have seen that the problem is to solve (2.3), subject to the conditions (2.4)-(2.5) and three other conditions still to be derived, in order to obtain the velocity field of the boundary as a function of time. The problem is ideally suited to be solved by a Boundary Element Method (Brebbia [2]). There we are only interested in the movement of the total region, thus only the velocity at the boundary is required. Hence, we shall represent the solution in terms of boundary distributions of the single- and double-layer potentials for the Stokes equation. In this form, we can directly calculate the shape and motion of our viscous body. From this we can derive the extra conditions, to ensure that the problem has a unique solution.

3.1 Extra conditions to make the problem solvable

We shall first derive the boundary integral formulation. Many authors attribute the analysis and the integral equation that follows to Ladyzhenskaya [12] (1963), but actually it was Lorentz [13] who derived this formulation in essence, back in 1896.
We introduce the fundamental solution $\mathbf{u}^k(\mathbf{x},\mathbf{y})$, $q^k(\mathbf{x},\mathbf{y})$ of the Stokes equations, i.e. the problem

$$\begin{aligned} \Delta \mathbf{u}^k(\mathbf{x},\mathbf{y}) - \operatorname{grad} \mathrm{q}^k(\mathbf{x},\mathbf{y}) &= \delta(\mathbf{x}-\mathbf{y})\mathbf{e}^k \\ \operatorname{div} \mathbf{u}^k &= 0, \end{aligned} \tag{3.1}$$

where k=1,2. Here $\mathbf{e}^k = (\delta_{1k}, \delta_{2k})$, with δ_{ij} the *Kronecker delta*, and $\delta(\mathbf{x}-\mathbf{y})$ is

the *Dirac delta function.* Furthermore, all differentiations are carried out with respect to the variable $\mathbf{x}$; the applied unit force is concentrated at the point $\mathbf{y}$. This problem can be solved uniquely using the requirement that $\mathbf{u}^k$ and q^k approach zero as $|\mathbf{x}| \to \infty$. For $\mathbf{u}^k$ and q^k we then obtain

$$\begin{aligned} u_j^k(\mathbf{x},\mathbf{y}) &= -\frac{1}{4\pi}\left[\delta_{jk}\log\frac{1}{|\mathbf{x}-\mathbf{y}|} + \frac{(x_j-y_j)(x_k-y_k)}{|\mathbf{x}-\mathbf{y}|^2}\right] \\ q^k(\mathbf{x},\mathbf{y}) &= -\frac{x_k-y_k}{2\pi|\mathbf{x}-\mathbf{y}|^2}. \end{aligned} \tag{3.2}$$

These functions $\mathbf{u}^k$ and q^k are also the solutions to the adjoint system (i.e. differentiation is carried out with respect to y)

$$\begin{aligned} \triangle_y \mathbf{u}^k(\mathbf{x},\mathbf{y}) + \operatorname{grad}_y \mathrm{q}^{\mathrm{k}}(\mathbf{x},\mathbf{y}) &= \delta(\mathbf{x}-\mathbf{y})\mathbf{e}^k \\ \operatorname{div}_y \mathbf{u}^{\mathrm{k}} &= 0. \end{aligned} \tag{3.3}$$

Since we are considering a Newtonian fluid flow, the stress tensor $\mathcal{T}(q,\mathbf{u})$ can be expressed as

$$\mathcal{T}_{ik}(q,\mathbf{u}) = -\delta_{ik}q + \left(\frac{\partial u_i}{\partial x_k} + \frac{\partial u_k}{\partial x_i}\right). \tag{3.4}$$

When we integrate the identity

$$\frac{\partial}{\partial x_k}\left[\mathcal{T}_{ik}(q,\mathbf{u})\right] = \frac{1}{2}\left(\frac{\partial u_i}{\partial x_k} + \frac{\partial u_k}{\partial x_i}\right)\left(\frac{\partial v_i}{\partial x_k} + \frac{\partial v_k}{\partial x_i}\right) + \left(\triangle u_i - \frac{\partial q_i}{\partial x_i}\right) v_i \tag{3.5}$$

over Ω, we obtain

$$\begin{aligned} \int_\Omega \left(\triangle u_i - \frac{\partial q_i}{\partial x_i}\right) v_i \, d\Omega &= -\tfrac{1}{2}\int_\Omega \left(\frac{\partial u_i}{\partial x_k} + \frac{\partial u_k}{\partial x_i}\right)\left(\frac{\partial v_i}{\partial x_k} + \frac{\partial v_k}{\partial x_i}\right) d\Omega \\ &\quad + \int_\Gamma \mathcal{T}_{ik}(q,\mathbf{u}) v_i n_k \, d\Gamma. \end{aligned} \tag{3.6}$$

By interchanging u_i and v_i in equation (3.6) and introducing an arbitrary smooth function p together with q, we obtain from equation (3.6)

$$\begin{aligned} \int_\Omega \left[\left(\triangle v_i - \frac{\partial p_i}{\partial x_i}\right) u_i - \left(\triangle u_i + \frac{\partial q_i}{\partial x_i}\right) v_i\right] d\Omega = \\ = \int_\Gamma \left[\mathcal{T}_{ij}(p,\mathbf{v}) u_i n_j - \mathcal{T}'_{ij}(q,\mathbf{u}) v_i n_j\right] d\Gamma \end{aligned} \tag{3.7}$$

where

$$\mathcal{T}'_{ij}(q,\mathbf{u}) = \delta_{ij}q + \left(\frac{\partial u_i}{\partial x_j} + \frac{\partial u_j}{\partial x_i}\right). \tag{3.8}$$

Note that equations (3.6) and (3.7) are the so-called *Green's formulae* corresponding to the Stokes problem. When we replace $\mathbf{u}$ and q with the fundamental singular solution $\mathbf{u}^k(\mathbf{x},\mathbf{y})$, $q^k(\mathbf{x},\mathbf{y})$ and note that these singular solutions, as a function of y, satisfy the adjoint system we obtain

$$v_k(\mathbf{x}) = \int_\Gamma \mathcal{T}'_{ij}(q^k, \mathbf{u}^k)_y v_i n_j \, d\Gamma_y - \int_\Gamma \mathcal{T}_{ij}(p, \mathbf{v}) u_i^k n_j \, d\Gamma_y \tag{3.9}$$

for any $\mathbf{x} \in \Omega$. By $(\,)_y$ we mean that the differentiation is carried out with respect to y. From equation (3.2) we find

$$\mathcal{T}'_{ij}(q^k, \mathbf{u}^k)_y = -\frac{(x_i - y_i)(x_j - y_j)(x_k - y_k)}{\pi |\mathbf{x} - \mathbf{y}|^4}, \tag{3.10}$$

and from equation (2.6) follows

$$\mathcal{T}_{ij}(p, \mathbf{v}) n_j = \kappa(\mathbf{y}) n_i, \tag{3.11}$$

where $\kappa(\mathbf{y})$ is the curvature of the boundary Γ at the point $\mathbf{y} \in \Gamma$.
In what follows we shall use *Greek letters* $\xi, \eta, ..$ to denote points on the boundary Γ. The boundary integrals in (3.9) are called hydrodynamical potentials of single- and double- layers (Ladyzhenskaya [12]). Following [12] we define the potential of a single layer with density $\psi(\eta)$ as

$$\mathrm{V}_i(\mathbf{x}, \psi) = -\int_\Gamma u_i^k(\mathbf{x}, \eta) \psi_k(\eta) \, d\Gamma_\eta. \tag{3.12}$$

By the potential of a double layer with density $\varphi(\eta)$ we mean

$$\begin{aligned} \mathrm{W}_k(\mathbf{x}, \varphi) &= \int_\Gamma \mathcal{T}'_{ij}(q^k, \mathbf{u}^k)_\eta \varphi_i(\eta) n_j(\eta) \, d\Gamma_\eta \\ &= \int_\Gamma K_{kj}(\mathbf{x}, \eta) \varphi_j(\eta) \, d\Gamma_\eta, \end{aligned} \tag{3.13}$$

where

$$K_{ij}(\mathbf{x}, \eta) = -\frac{(x_i - \eta_i)(x_j - \eta_j)(x_k - \eta_k)}{\pi |\mathbf{x} - \eta|^4} n_k(\eta). \tag{3.14}$$

From equation (3.9) We now obtain for $\mathbf{x} \in \Omega$:

$$v_k(\mathbf{x}) = W_k(\mathbf{x}, \mathbf{v}) + V_k(\mathbf{x}, \kappa \mathbf{n}). \tag{3.15}$$

Assuming the boundary Γ is "smooth", it can be seen, see [12], that for a point $\mathbf{x} = \xi$ on Γ the velocity vector $\mathbf{v}(\xi)$ is given by

$$\frac{1}{2} v_k(\xi) = W_k(\xi, \mathbf{v}) + V_k(\xi, \kappa \mathbf{n}). \tag{3.16}$$

The factor 1/2 is caused by the "jump" of the double-layer potential $\mathbf{W}_k(\xi, \mathbf{v})$. This latter equation will be used to solve the viscous sintering problem.
Before doing this we shall investigate the number of degrees of freedom which equation (3.16) still has. As mentioned in section 2, this must be three. To derive this we consider both $\mathbf{v}^1$ and $\mathbf{v}^2$ to be solutions to equation (3.16). For the difference $\varphi = \mathbf{v}^1 - \mathbf{v}^2$ we can derive the following equation

$$-\frac{1}{2} \varphi_i(\xi) + \int_\Gamma K_{ij}(\xi, \eta) \varphi_j(\eta) \, d\Gamma_\eta = 0. \tag{3.17}$$

For the solution to equation (3.17) we now propose the following lemma:

LEMMA 1: *Equation (3.17) possesses three linearly independent solutions* φ^k *with*

$$\varphi^k(\mathbf{x}) = (\delta_{1k}, \delta_{2k}) = \mathbf{e}^k \qquad k = 1,2$$
$$\varphi^3(\mathbf{x}) = (x_2, -x_1).$$

Proof: This lemma can be proven in the following way. First we show that these $\varphi^k(\mathbf{x})$ are solutions to equation (3.17). Consider therefore any of the vectors $\varphi^k(\mathbf{x})$ and a smooth function p^k, which will satisfy the homogeneous system

$$\begin{aligned} \Delta\varphi^k - \operatorname{grad} \mathrm{p}^{\mathrm{k}} &= 0 \\ \operatorname{div} \varphi^{\mathrm{k}} &= 0, \end{aligned} \tag{3.18}$$

i.e. for example, take $p^k(\mathbf{x}) \equiv 0$.
Furthermore, we note that from equation (3.4) it follows that $\mathcal{T}_{ij}(p^k, \varphi^k) \equiv 0$. We now derive from equation (3.9):

$$\varphi_i^k(\mathbf{x}) = W_i(\mathbf{x}, \varphi^k) \qquad \mathbf{x} \in \Omega. \tag{3.19}$$

By letting $\mathbf{x}$ approach $\xi \in \Gamma$ it can be derived that (Ladyzhenskaya [12])

$$W_i(\xi, \varphi^k) = \frac{1}{2}\varphi_i^k(\xi) + \int_\Gamma K_{ij}(\xi, \eta)\varphi_j^k(\eta)\, d\Gamma_\eta. \tag{3.20}$$

From equation (3.19) we thus obtain for $\mathbf{x} \to \xi$

$$\varphi_i^k(\xi) = \frac{1}{2}\varphi_i^k(\xi) + \int_\Gamma K_{ij}(\xi, \eta)\varphi_j^k(\eta)\, d\Gamma_\eta. \tag{3.21}$$

So $\varphi^k(\xi)$ is actually a solution to the system (3.17). Furthermore, we must show that any other solution φ to equation (3.17) depends linearly on φ^k. This part of the proof is rather technical and can be found in Ladyzhenskaya [12], even for the 3-D case; for the 2-D problem this proof is a straightforward analogue of [12]. □

A physical interpretation of this lemma can be given as follows: $\varphi^1(\xi)$ and $\varphi^2(\xi)$ describe a rigid-body translation of Ω in the $\mathbf{e}^1$- and $\mathbf{e}^2$-direction, respectively; $\varphi^3(\xi)$ also gives a rigid-body movement but this is a rotation over $\pi/4$ rad. Thus when we want to solve the viscous sintering problem, we must include three extra conditions in our problem to ensure that the solution is unique.
From equation (3.19) it follows that $\varphi^k(\mathbf{x})$ is also a solution when $\mathbf{x} \in \Omega$. Thus we can represent the general velocity solution $\bar{\mathbf{v}}$ of our viscous sintering problem by

$$\begin{aligned} \bar{v}_1(\mathbf{x}) &= v_1(\mathbf{x}) + \alpha_1 x_2 + \alpha_2 \\ \bar{v}_2(\mathbf{x}) &= v_2(\mathbf{x}) - \alpha_1 x_1 + \alpha_3 \end{aligned} \tag{3.22}$$

where α_1, α_2 and $\alpha_3 \in \Re$. We want to fix these 3 numbers. We can achieve this as follows.

For the rotation-operator on $\bar{\mathbf{v}}$ in 2-D, we have

$$\mathrm{rot}\bar{\mathbf{v}}(\mathbf{x}) = \frac{\partial \mathrm{v}_2}{\partial \mathrm{x}_1} - \frac{\partial \mathrm{v}_1}{\partial \mathrm{x}_2} - 2\alpha_1 \qquad \mathbf{x} \in \Omega. \tag{3.23}$$

When we assume no internal rotation of the fluid flow then

$$\mathrm{rot}\mathbf{v}(\mathbf{x}) = 0 \qquad \mathbf{x} \in \Omega. \tag{3.24}$$

So also $\mathrm{rot}\bar{\mathbf{v}} \equiv 0$, thus $\alpha_1 = 0$. When we integrate equation (3.24) over Ω and using Stokes's theorem, we find

$$\int_\Gamma (\mathbf{v}, \tau)\, d\Gamma = 0, \tag{3.25}$$

where τ is the tangential vector of the boundary Γ.
In order to get rid of the translation component, we formulate the problem to be stationary at a (reference) point in the fluid: $\mathbf{x}^r$. The most natural choice for this reference point is the centre of mass: the point where the gravity forces grips the body, thus:

$$\mathbf{v}(\mathbf{x}^r) = 0. \tag{3.26}$$

3.2 Boundary problem formulation

As mentioned before, the viscous sintering problem is governed by the equations (3.15) and (3.16). Recall that for an *arbitrary* point $\mathbf{x}$ of the body Ω, we can express the velocity v_k, using indicial notation, in the general 2D-form:

$$\begin{aligned} c_{kj}v_j + \int_\Gamma \frac{(x_i - \eta_i)(x_j - \eta_j)(x_k - \eta_k)}{\pi |\mathbf{x} - \eta|^4} v_i n_j \, d\Gamma_\eta \qquad &= \\ = \frac{1}{4\pi} \int_\Gamma \Big[\delta_{ik} \log \frac{1}{|\mathbf{x} - \eta|} + \frac{(x_i - \eta_i)(x_k - \eta_k)}{|\mathbf{x} - \eta|^2} \Big] \mathcal{T}_{ij}(p, \mathbf{v}) n_j \, d\Gamma_\eta, & \end{aligned} \tag{3.27}$$

where

$$c_{ij} = \begin{cases} \delta_{ij} & \text{when } \mathbf{x} \in \Omega; \\ \frac{1}{2}\delta_{ij} & \text{when } \mathbf{x} \in \Gamma \quad \text{and } \Gamma = \text{“}smooth\text{”}. \end{cases}$$

κn_i (cf. (3.11)) is written as

$$b_i = \mathcal{T}_{ij}(p, \mathbf{v}) n_j \Big|_\Gamma = \kappa n_i. \tag{3.28}$$

From (3.27) we then find the following matrix equation related to the point $\mathbf{x}$:

$$\mathcal{C}\mathbf{v}(\mathbf{x}) + \int_\Gamma \mathcal{Q}\mathbf{v} \, d\Gamma_\eta = \int_\Gamma \mathcal{U}\mathbf{b} \, d\Gamma_\eta, \tag{3.29}$$

where $\mathcal{C}$,$\mathcal{Q}$ and $\mathcal{U}$ are 2×2 matrices with coefficients c_{ij}, q_{ij} and u_{ij} respectively:

$$q_{ij} = \frac{r_i r_j}{\pi R^4} r_k n_k \tag{3.30}$$

$$u_{ij} = \frac{1}{4\pi}\Big[\,\delta_{ij}\log\frac{1}{R} + \frac{r_i r_j}{R^2}\,\Big], \tag{3.31}$$

where $r_i = x_i - \eta_i$ and $\mathrm{R}=\sqrt{r_1^2 + r_2^2} = |\mathrm{x} - \eta|$.
We also have to account for the fact that the velocity of our chosen reference point $\mathbf{x}^r$ in Ω is zero, to ensure that equation (3.29) has a unique solution:

$$\int_\Gamma \mathcal{Q}^r \mathbf{v}\, d\Gamma_\eta = \int_\Gamma \mathcal{U}^r \mathbf{b}\, d\Gamma_\eta, \tag{3.32}$$

where $\mathcal{Q}^r = \mathcal{Q}^r(\mathbf{x}^r, \eta)$ and $\mathcal{U}^r = \mathcal{U}(\mathbf{x}^r, \eta)$.
From equation (3.29) and (3.32) we obtain

$$\mathcal{C}\mathbf{v}(\mathbf{x}) + \int_\Gamma (\mathcal{Q} - \mathcal{Q}^r)\mathbf{v}\, d\Gamma_\eta = \int_\Gamma (\mathcal{U} - \mathcal{U}^r)\mathbf{b}\, d\Gamma_\eta. \tag{3.33}$$

Furthermore, we want our viscous body to be rotation-free, cf. (3.25); so

$$\int_\Gamma (\mathbf{v}, \tau)\, d\Gamma \;=\; 0. \tag{3.34}$$

Thus, to determine the unknown velocity at the boundary we apply the general solution (3.33) *at* the boundary, i.e. $\mathbf{x} = \xi \in \Gamma$, and condition (3.24), to ensure that the solution is unique.

4 Numerical Solution

4.1 The Boundary Element Method

We shall use the Boundary Element Method (BEM) to solve the integral equations (3.33)-(3.34). For this, the boundary has to be discretized into a sequence of elements where the velocity and the surface tension are written in terms of their values at a sequence of nodal points. From the discretized form of (3.33) for every nodal point and the extra condition (3.34), we obtain a system of (2N+1) linear algebraic equations with 2N unknowns. This system gives a unique approximate solution of the velocity field, and so from equation (2.5) a new boundary can be obtained.
After dividing the boundary Γ into N elements, we define functions $\mathbf{v}$ and $\mathbf{b}$ which apply at a typical element 'j',

$$\begin{aligned} \mathbf{v} &= \Phi v^j \\ \mathbf{b} &= \Phi b^j, \end{aligned} \tag{4.1}$$

where v^j and b^j are the element nodal velocity and surface tension. The interpolation function Φ is a $2 \times 2M$ matrix of shape functions:

$$\Phi = \begin{bmatrix} \phi_1 & 0 & \phi_2 & 0 & \dots & \phi_M & 0 \\ 0 & \phi_1 & 0 & \phi_2 & \dots & 0 & \phi_M \end{bmatrix} = [\Phi_1\ \Phi_2\ \dots\ \Phi_M]. \tag{4.2}$$

These functions are the standard finite-element-type functions (Brebbia [2]). We substitute the functions (4.1) and (4.2) into equation (3.33) and discretize the boundary. We derive the following equation for an *arbitrary* nodal point i:

$$\mathcal{C}^i v^i + \sum_{j=1}^{N} \Big(\int_{\Gamma_j} (\mathcal{Q} - \mathcal{Q}^r)\Phi \, d\Gamma_\eta \Big) v^j = \sum_{j=1}^{N} \Big(\int_{\Gamma_j} (\mathcal{U} - \mathcal{U}^r)\Phi \, d\Gamma_\eta \Big) b^j. \tag{4.3}$$

Note that $\mathcal{C}^i$=0.5 for a "smooth" boundary, i.e. constant elements: **v**, **b** are assumed to be constant over each element. Otherwise, for higher-order elements $\mathcal{C}$ will be a 2×2 matrix.
The following types of integrals have to be evaluated element-wise

$$\begin{aligned} \hat{H}^{ij} &= \int_{\Gamma_j} \mathcal{Q}\Phi \, d\Gamma_\eta; \qquad & H_r^j &= \int_{\Gamma_j} \mathcal{Q}^r \Phi \, d\Gamma_\eta \\ G^{ij} &= \int_{\Gamma_j} \mathcal{U}\Phi \, d\Gamma_\eta; \qquad & G_r^j &= \int_{\Gamma_j} \mathcal{U}^r \Phi \, d\Gamma_\eta. \end{aligned} \tag{4.4}$$

Hence at a particular point, i say, we can write for equation (4.3):

$$\mathcal{C}^i v^i + \sum_{j=1}^{N} \Big(\hat{H}^{ij} - H_r^j \Big) v^j = \sum_{j=1}^{N} \Big(G^{ij} - G_r^j \Big) b^j. \tag{4.5}$$

If we now let i vary from 1 to N and set

$$H^{ij} = \begin{cases} \hat{H}^{ij} & i \neq j \\ \hat{H}^{ij} + \mathcal{C}^i & i = j, \end{cases} \tag{4.6}$$

then we obtain from (4.5)

$$\sum_{j=1}^{N} \Big(H^{ij} - H_r^j \Big) v^j = \sum_{j=1}^{N} \Big(G^{ij} - G_r^j \Big) b^j. \tag{4.7}$$

As was pointed out, the diagonal submatrices H^{ii} include terms in $\hat{H}^{ij}$ and $\mathcal{C}^i$. Difficulties appear when trying to compute these terms explicitly; particularly at corners where the fundamental solution has a singularity. Assume the whole body has a velocity **v** in the direction of one of the Cartesian coordinates and note that the curvature vector **b** does not change. Then we can obtain the following equation:

$$\mathcal{H}e = 0 \ \text{ with } \ e = (1, \dots, 1) \ \text{ or : } \ H^{ii} = -\sum_{\substack{j=1 \\ j \neq i}}^{N} H^{ij}. \tag{4.8}$$

4.2 The computation of the curvature

As mentioned before, the driving force of the sintering problem is a tension that depends on the surface energy of the boundary and its geometry, i.e. (2.4). A local method is used to determine the curvature κ at the nodal points of the boundary. This curvature is found by fitting a quadratic polynomial at the nodal point, say η^2, and its two neighbours η^1 and η^3. For the quadratic polynomial we can write

$$\eta(s) = \eta^1\phi_1(s) + \eta^2\phi_2(s) + \eta^3\phi_3(s), \tag{4.9}$$

where $\phi_1(s) = \frac{1}{2}s(s-1)$; $\phi_2(s) = 1 - s^2$; $\phi_2(s) = \frac{1}{2}s(s+1)$.
For the curvature at $\eta^2 = \eta(s=0)$, we can derive:

$$\begin{aligned} \kappa(\eta^2) &= \frac{(\eta_2)_s(\eta_1)_{ss} - (\eta_1)_s(\eta_2)_{ss}}{\left(((\eta_1)_s)^2 + ((\eta_2)_s)^2\right)^{\frac{3}{2}}} \\ &\doteq \frac{4\left[(\eta_2^3 - \eta_2^1)(\eta_1^1 - 2\eta_1^2 + \eta_1^3) - (\eta_1^3 - \eta_1^1)(\eta_2^1 - 2\eta_2^2 + \eta_2^3)\right]}{((\eta_1^3 - \eta_1^1)^2 + (\eta_2^3 - \eta_2^1)^2)^{\frac{3}{2}}}. \end{aligned} \tag{4.10}$$

Furthermore, we make a linear fit through these nodal curvatures to determine the curvature at any point of the element, especially the integration points.
When computing the curvature, the following problems occur. In a point where a cusp arises, the curvature becomes unbounded. Thus the approximate curvature in such a point can have large errors. Furthermore, when we refine too much in the neighbourhood of such a point, we make large errors when computing the curvature using the above formula. This is because both the numerator and the denominator in (4.10) approach zero. This is a serious problem, which we shall illustrate by an example. Assume that the spatial discretization error is smaller than the time discretization error. This is justified by the fact that we use a simple forward Euler scheme for computing the moving boundary (see section 4.3), so the global time discretization error is $\mathcal{O}(\Delta\tau)$. We cannot make the time step $\Delta\tau$ very small, because then the total computing time will become prohibitively large. Thus we may say that the computed boundary deviates $\mathcal{O}(\Delta\tau)$ from the exact curve. When we approximate the curvature at points where the mesh is fine, we loose some accuracy because some points are necessarily very close to each other. The quotient at the right-hand side of equation (4.10) will then be of the order $\Delta\tau$ over order $\Delta\tau$. Hence the computed curvature can deviate considerably from the exact curvature and soon oscillations will develop. These oscillations result from the following feedback cycle: (1) small errors in the approximate collocation points produce (2) local variations in the computed velocities of the collocation points, causing (3) uneven advancement of these points which yields (4) larger errors in the approximation. This process can lead to instabilities and wrong curves and even a complete breakdown of the algorithm. To be more specific, consider a situation of sintering spheres in 2-D, fairly shortly after they

have made contact (so there still is an almost cusp like-part of the boundary). Let (η_1^i, η_2^i) be some points at the boundary curve, $\kappa(\eta^i)$ the approximate curvature and let $\Delta\tau = 0.001$. We then obtain numerical results as shown in Table 4.1.

i	η_1^i	η_2^i	$\kappa(\eta^i)$
1	0.24576958	0.00000000	121.74770396
2	0.24635812	0.00310939	96.11441305
3	0.24813714	0.00629589	54.81639820
4	0.25114742	0.00964125	28.04820956
⋮	⋮	⋮	⋮

Table 4.1

For the approximation of the curvature, e.g. in η^2, we must compute

$$\begin{array}{lcll} \eta_1^3 - \eta_1^1 & = & 0.00236756 & \text{2 digits lost and of } \mathcal{O}(\Delta\tau); \\ \eta_2^3 - \eta_2^1 & = & 0.00629589 & \text{exact;} \\ \eta_1^1 - 2\eta_1^2 + \eta_1^3 & = & 0.00119048 & \text{2 digits lost and of } \mathcal{O}(\Delta\tau); \\ \eta_2^1 - 2\eta_2^2 + \eta_2^3 & = & 0.00007711 & \text{2 digits lost and of } \mathcal{O}(\Delta\tau); \end{array}$$

This clearly demonstrates that the approximation for $\kappa(\eta^2)$ as found from (4.10) may be $\mathcal{O}(\Delta\tau)$ over $\mathcal{O}(\Delta\tau)$; nevertheless it often works satisfactorily. We plan to investigate better time-stepping schemes in the future.

4.3 The linear element solution

We consider a linear variation of $\mathbf{v}$ and $\mathbf{b}$ over an element, the nodal points at the end. As we saw in (4.1), the values of $\mathbf{v}$ and $\mathbf{b}$ at any point of the element can be expressed in terms of their nodal values and two linear interpolation functions ϕ_1 and ϕ_2, which are given in the form of the basis-free coordinate s as,

$$\begin{aligned} \phi_1 &= \tfrac{1}{2}(1-s) \\ \phi_2 &= \tfrac{1}{2}(1+s). \end{aligned} \tag{4.11}$$

Furthermore, the boundary can be expressed in terms of functions of the same interpolations:

$$\begin{aligned} \eta &= \Phi\eta^j \\ &= \tfrac{1}{2}(\eta^2 - \eta^1)\, s \;+\; \tfrac{1}{2}(\eta^1 + \eta^2). \end{aligned} \tag{4.12}$$

Here η^1, η^2 are the coordinates of the nodal points of the element under consideration.

In an similar way as described in section 4.1, we derive equation (4.7) for the discretized form of (3.33). The submatrices found in (4.7), i.e. $\hat{H}^{ij}$, H_r^j, G^{ij} and G_r^j are now 2×4 matrices. The integrals are then of a type as in (4.4). From (4.12) we find that these integrals are of the following type:

$$\int_{-1}^{1} \phi_k u_{lm} |J| \, ds; \quad \text{or} \quad \int_{-1}^{1} \phi_k q_{lm} |J| \, ds. \tag{4.13}$$

Where $|J|$ is the Jacobian, i.e.

$$|J| = \sqrt{\left(\frac{\partial \eta_1}{\partial s}\right)^2 + \left(\frac{\partial \eta_2}{\partial s}\right)^2} = \frac{1}{2}|\eta^2 - \eta^1|. \tag{4.14}$$

For the outward normal $\mathbf{n}$ we find

$$\mathbf{n} = \frac{1}{|J|} \begin{pmatrix} -a_2 \\ a_1 \end{pmatrix}, \tag{4.15}$$

where $a_i = \frac{1}{2}(\eta_i^1 - \eta_i^2)$.
Further analysis of (4.13) gives the following eight integrals which are to be computed for each element with index j, say, with nodal points η^1 and η^2, related to the node ξ^i.

$$\begin{aligned}
I_1^G(\gamma) &= \int_{-1}^{1} (1+\gamma s) \frac{r_1^2}{R^2} \, ds & I_2^G(\gamma) &= \int_{-1}^{1} (1+\gamma s) \frac{r_2^2}{R^2} \, ds \\
I_3^G(\gamma) &= \int_{-1}^{1} (1+\gamma s) \frac{r_1 r_2}{R^2} \, ds & I_4^G(\gamma) &= \int_{-1}^{1} (1+\gamma s) \log |R^2| \, ds \\
I_1^H(\gamma) &= \int_{-1}^{1} (1+\gamma s) \frac{r_1^3}{R^4} \, ds & I_2^H(\gamma) &= \int_{-1}^{1} (1+\gamma s) \frac{r_2^3}{R^4} \, ds \\
I_3^H(\gamma) &= \int_{-1}^{1} (1+\gamma s) \frac{r_1^2 r_2}{R^4} \, ds & I_4^H(\gamma) &= \int_{-1}^{1} (1+\gamma s) \frac{r_1 r_2^2}{R^4} \, ds,
\end{aligned} \tag{4.16}$$

where $\gamma = \pm 1$;

$r_j = a_j s + b_j$ with $b_j = \frac{1}{2}(2\xi_j^i - \eta_j^1 - \eta_j^2)$.

We note that

$$I_1^G(\gamma) + I_2^G(\gamma) = \int_{-1}^{1} (1+\gamma s) \, ds = 2. \tag{4.17}$$

Thus in total we need to evaluate fourteen integrals for each element 'j' and nodal point ξ^i. From the integrals I_j^G, I_j^H we derive the 2×4 submatrices G^{ij} and $\hat{H}^{ij}$, respectively. The integrals of (4.16) are related to these submatrices as follows,

$$
\begin{aligned}
(\mathrm{G}^{ij})_{11} &= \int_{-1}^{1} \phi_1 u_{11} |\mathrm{J}|\, ds &&= \frac{|\mathrm{J}|}{8\pi}\left[\, \mathrm{I}_1^G(-1) \;-\; \tfrac{1}{2}\mathrm{I}_4^G(-1)\,\right] \\
(\mathrm{G}^{ij})_{12} &= \int_{-1}^{1} \phi_1 u_{12} |\mathrm{J}|\, ds &&= \frac{|\mathrm{J}|}{8\pi}\, \mathrm{I}_3^G(-1) \\
(\mathrm{G}^{ij})_{21} &= (\mathrm{G}^{ij})_{12} \\
(\mathrm{G}^{ij})_{22} &= \int_{-1}^{1} \phi_1 u_{22} |\mathrm{J}|\, ds &&= \frac{|\mathrm{J}|}{8\pi}\left[\, \mathrm{I}_2^G(-1) \;-\; \tfrac{1}{2}\mathrm{I}_4^G(-1)\,\right] \\
(\mathrm{H}^{ij})_{11} &= \int_{-1}^{1} \phi_1 q_{11} |\mathrm{J}|\, ds &&= \frac{1}{2\pi}\left[\, a_2 \mathrm{I}_1^H(-1) \;-\; a_1 \mathrm{I}_3^H(-1)\,\right] \\
(\mathrm{H}^{ij})_{12} &= \int_{-1}^{1} \phi_1 q_{12} |\mathrm{J}|\, ds &&= \frac{1}{2\pi}\left[\, a_2 \mathrm{I}_3^H(-1) \;-\; a_1 \mathrm{I}_4^H(-1)\,\right] \\
(\mathrm{H}^{ij})_{21} &= (\mathrm{H}^{ij})_{12} \\
(\mathrm{H}^{ij})_{22} &= \int_{-1}^{1} \phi_1 q_{22} |\mathrm{J}|\, ds &&= \frac{1}{2\pi}\left[\, a_2 \mathrm{I}_4^H(-1) \;-\; a_1 \mathrm{I}_2^H(-1)\,\right].
\end{aligned}
\tag{4.18}
$$

A similar expression can be found for the elements $(\mathrm{G}^{ij})_{l,2+k}$ and $(\hat{H}^{ij})_{l,2+k}$ when the interpolation function is ϕ_2, i.e. when $\gamma = 1$.
The integrals of (4.16) are computed using a four-point Gauss quadrature formula. However, when $\xi^i = \eta^1$ or $\xi^i = \eta^2$, i.e. the nodal point ξ^i lies in the element considered, the integrals have a singularity. Because of this singularity, the four-point Gauss formula used for the approximation of these integrals will not give satisfactory results. The approximations can involve large errors in the submatrices G^{ii} and $\hat{H}^{ii}$. We therefore compute these integrals analytically. This can be done easily for the integrals I_j^G and I_j^H, note that here $r_i = a_i(1+s)$ or $r_i = a_i(1-s)$ when $\xi = \eta^1$ or $\xi = \eta^2$, respectively, hence we obtain:

$$
\begin{aligned}
\mathrm{I}_j^H(\gamma) &= 0 \qquad \text{for } j = 1, \ldots, 4 \\
\mathrm{I}_1^G(\gamma) &= \frac{2a_1^2}{a_1^2 + a_2^2} \\
\mathrm{I}_2^G(\gamma) &= \frac{2a_2^2}{a_1^2 + a_2^2} \\
\mathrm{I}_3^G(\gamma) &= \frac{2a_1 a_2}{a_1^2 + a_2^2} \\
\mathrm{I}_4^G(\gamma) &= 2\log(a_1^2 + a_2^2) \;+\; 2\int_{-1}^{1} (1 + \gamma s)\log(s \pm 1)\, ds \\
&= \begin{cases}
2[\log(4(a_1^2 + a_2^2)) - 1] \;\text{ if } \begin{cases} \gamma = 1 \\ \xi^i = \eta^1 \end{cases} \text{ or } \begin{cases} \gamma = -1 \\ \xi^i = \eta^2 \end{cases} \\
2[\log(4(a_1^2 + a_2^2)) - 3] \;\text{ if } \begin{cases} \gamma = 1 \\ \xi^i = \eta^2 \end{cases} \text{ or } \begin{cases} \gamma = -1 \\ \xi^i = \eta^1. \end{cases}
\end{cases}
\end{aligned}
\tag{4.19}
$$

Furthermore, note that $\mathbf{b}$ is a known vector, thus $G^{ij}b^j$ is a (sub) vector which we denote by F^j. For F^j we find:

$$F_k^j = \kappa^j \left((G^{ij})_{k1} n_1 + (G^{ij})_{k2} n_2 \right) + \kappa^{j+1} \left((G^{ij})_{k3} n_1 + (G^{ij})_{k4} n_2 \right). \quad (4.20)$$

As mentioned before, for *every* nodal point ξ^i and for *each* element we must compute the integrals of (4.16), to obtain the system matrix $\mathcal{H}$ and the right-hand vector $\mathbf{F}$. By $\mathcal{H}$ we mean the $2N \times 2N$ matrix derived from the submatrices H^{ij}. The 2×2 diagonal blocks of $\mathcal{H}$ are computed using the rigid-body considerations as derived before, i.e. (4.8). To obtain the discretized form of (4.7), we also need to compute (once) the integrals of (4.16) over every element when $\xi = \mathbf{x} \in \Omega$ is the reference point $\mathbf{x}^r$. So we obtain the submatrices G_r^j and H_r^j. Again, we can replace the submatrix G_r^j by the subvector F_r^j. In this way, we obtain a $2 \times 2N$ matrix H_r and a 2-vector F_r. To $\mathcal{H}$ and $\mathbf{F}$ we apply the following operations, for obtaining the system of (3.33):

$$\begin{array}{rcll} \mathcal{H}_k & = & \mathcal{H}_{k-1} - \mathcal{M}_k^r & \\ \mathbf{F}_k & = & \mathbf{F}_{k-1} - \mathbf{D}_k^r & \text{for } k = 0, ..., \mathrm{N}-1 \end{array} \quad (4.21)$$

where

$$\mathcal{H}_{-1} = \mathcal{H} \text{ and } \mathbf{F}_{-1} = \mathbf{F};$$

$$\mathcal{M}_k = \underbrace{\begin{bmatrix} 0 \\ \mathrm{H}_r \\ 0 \end{bmatrix}}_{2N} \begin{matrix} \updownarrow \\ \updownarrow \\ \updownarrow \end{matrix} \begin{matrix} 2k \\ 2 \\ 2(N-k-1) \end{matrix} \quad \text{and} \quad \mathbf{D}_k = \underbrace{\begin{bmatrix} 0 \\ \mathbf{F}_r \\ 0 \end{bmatrix}}_{1} \begin{matrix} \updownarrow \\ \updownarrow \\ \updownarrow \end{matrix} \begin{matrix} 2k \\ 2 \\ 2(N-k-1) \end{matrix}$$

Denote the resulting matrix $\mathcal{H}_{N-1}$ by $\mathcal{H}_r$ and the resulting vector $\mathbf{F}_{N-1}$ by $\mathbf{F}_r$. The system

$$\mathcal{H}_r \mathbf{v} = \mathbf{F}_r \quad (4.22)$$

covers exactly equation (4.7). The matrix $\mathcal{H}_r$ has rank $2N-1$, thus (4.22) does not have a unique solution. To obtain a system with full column rank, we must include the extra condition that our body is rotation-free, i.e. equation (3.34). The integrals involved are easy to compute, in an similar way as was done above. This condition gives an extra row for the matrix $\mathcal{H}_r$, so the new $\mathcal{H}_r$ is a $(2\mathrm{N}+1) \times 2\mathrm{N}$ matrix.

This system (4.22) is solved by Gaussian elimination. The LU-decomposition of $\mathcal{H}_r$ is performed with partial pivoting. $\mathcal{H}_r$ has full column rank, so the last row of the upper triangular matrix $\mathcal{U}$ can be ignored for the backward substitution, and the system can be solved uniquely. However, when the reference point is not the centre of mass, the problem to solve is really a least-squares problem, which

is solved using a QU-decomposition.
The solution v is the approximate velocity field at time $\tau = \tau_k$ in the nodal boundary points ξ^i. The displacement of the boundary at time $\tau = \tau_{k+1} = \tau_k + \Delta\tau$ can be obtained by discretization of (2.5). Here we use a simple forward Euler discretization scheme, i.e.

$$\xi^i(\tau_{k+1}) = \xi^i(\tau_k) + \Delta\tau \mathbf{v}(\xi^i(\tau_k)). \tag{4.23}$$

By starting the numerical process at $\tau = \tau_0 = 0$, we set $\Delta\tau$ equal to $\Delta\tau_{\min}$. For $\tau > 0$ we obtain the $\Delta\tau$ from the following equation:

$$\Delta\tau = \min\left(\Delta\tau_{\max}, \max(\Delta\tau_{\min}, \Delta\tau^*)\right) \tag{4.24}$$

where $\Delta\tau^*$ is defined as:

$$\Delta\tau^* = C\sqrt{\frac{\Delta\tau_{old}}{\max_{i=1}^{N} | \, |\mathbf{v}(\xi^i(\tau_{k+1}))| - |\mathbf{v}(\xi^i(\tau_k))| \, |}} \tag{4.25}$$

and C is a constant.

4.4 Automatic mesh selection

When we the approximate of the boundary curve Γ with a polygon, an error is made. We need an easy criterion to monitor this error, so that we can insert or remove collocation points when necessary. A reasonable criterion would seem to be that the straight line between two contiguous collocation points should not deviate too much, in a relative sense, from that part of Γ which lies between those points. We denote the maximum deviation of element j and the boundary by h_j, and the length of the element j by δ_j. Then h_j/δ_j must be bounded above by a certain threshold value ϵ, i.e.

$$h_j < \epsilon\delta_j. \tag{4.26}$$

It is too expensive to compute this h_j for every element exactly, and after all we don't need to know this h_j exactly. An approximation of h_j is enough, as this gives an indication of where the polygon does not approximate the boundary well, and thus some action needs to be taken.
Suppose that η_1 and η_2 are two successive collocation points with curvature $\kappa(\eta^1)$ and $\kappa(\eta^2)$ respectively, as derived in section 4.2. An arc of the circle through η_1 and η_2 can be defined uniquely when the curvature, say κ^c, of this circle is given. Note that the radius r of this circle can found with the equation $r = 1/|\kappa^c|$. The maximum deviation of this circle with the straight line through η_1 and η_2 can then easily be found,

$$h_j^i = \frac{1}{|\kappa(\eta^i)|}\left(1 - \sqrt{1 - \frac{1}{4}\delta_j^2(\kappa(\eta^i))^2}\right) \qquad i = 1, 2. \tag{4.27}$$

Note that when $\kappa(\eta^i) \to 0$, it can be seen that $h_j^i \to 0$; i.e. the curve is a straight line. When $\kappa(\eta^i) > 2/\delta_j$, no solution can be found because the length of the element is too large to define an arc of the circle through η_1 and η_2.
Since the boundary curve Γ is sufficiently 'smooth' and from the curvature over an element is approximated by a linear function, the maximum deviation h_j of a straight line through η_1 and η_2 is bounded by the maximum of equation (4.27). Thus,

$$h_j < \max\left(h_j^1, h_j^2\right) \tag{4.28}$$

and so our criterion will be

$$\max\left(h_j^1, h_j^2\right) < \delta_j \epsilon. \tag{4.29}$$

4.5 The quadratic element solution

We consider a quadratic variation of $\mathbf{v}$ and $\mathbf{b}$ over an element. Here three successive collocation points define the element. As mentioned in (4.1), the values of $\mathbf{v}$ and $\mathbf{b}$ at any point of the element can be expressed in terms of their nodal values and three quadratic interpolation functions ϕ_1, ϕ_2 and ϕ_3, e.g. section 4.2. In a way similar to that described in section 4.3, we find the discretized form. Note that the submatrices are now 2×6 matrices. We find for the integrals which are to be considered, that they are of the following type:

$$\int_{-1}^{1} \phi_k u_{lm} |\mathrm{J}|\, ds; \text{ or } \int_{-1}^{1} \phi_k q_{lm} |\mathrm{J}|\, ds. \quad \text{where } k = 1,.,3 \text{ and } l, m = 1, 2. \tag{4.30}$$

Where $|\mathrm{J}|$ is the Jacobian, i.e.

$$|\mathrm{J}| = \sqrt{(2a_1 s + b_1)^2 + (2a_2 s + b_2)^2} \tag{4.31}$$

where $a_i = -\frac{1}{2}(\eta_i^1 - 2\eta_i^2 + \eta_i^3)$
$b_i = -\frac{1}{2}(\eta_i^3 - \eta_i^1)$.

For the outward normal $\mathbf{n}$ we find

$$\mathbf{n} = \frac{1}{|\mathrm{J}|} \begin{pmatrix} -2a_2 s - b_2 \\ 2a_1 s + b_1 \end{pmatrix}. \tag{4.32}$$

The integrals which are to be computed for each element with index j, say, with nodal points η^1, η^2 and η^3, related to the node ξ^i are

$$
\begin{aligned}
(\mathrm{G}^{ij})_{2k-2+l,m} &= \frac{1}{4\pi}\int_{-1}^{1}\phi_k\left[\delta_{ij}\log\frac{1}{R}+\frac{r_l r_m}{R^2}\right]|\mathrm{J}|\,ds \\
(\mathrm{H}^{ij})_{2k-2+l,m} &= \frac{1}{\pi}\int_{-1}^{1}\phi_k\frac{r_l r_m}{R^4}\,\psi(s)\,ds,
\end{aligned}
\tag{4.33}
$$

where $k = 1,..,3$ and $l,m=1,..,2.$ and

$r_j = a_j s^2 + b_j s + c_j$ with $c_j = \frac{1}{2}(\xi_j^i - \eta_j^2)$

and $\psi(s) = (r_1 n_1 + r_2 n_2)\,|\mathrm{J}|$

$= (a_1 b_2 - a_2 b_1)\,s^2 + (a_1 c_2 - a_2 c_1)\,s + (b_1 c_2 - b_2 c_1)\,.$

The integrals of (4.33) are computed using a four-point Gauss quadrature formula. However, when $\xi^i = \eta^1$, η^2 or η^3, i.e. the nodal point ξ^i lies in the element considered, these integrals have a singularity. This singularity can easily be removed after some analytical manipulation. The integrals then become

$$
\begin{aligned}
(\mathrm{G}^{ii})_{2k-2+l,m} &= \frac{1}{4\pi}\left[\mathrm{I}_k^{\mathrm{G}} - \gamma\log 2\int_{-1}^{1}\phi_k\,|\mathrm{J}|\,ds + \right. \\
&\qquad \left. \int_{-1}^{1}\phi_k\left[\delta_{ij}\log\frac{1}{\tilde{R}}+\frac{\tilde{r}_l\tilde{r}_m}{\tilde{R}^2}\right]|\mathrm{J}|\,ds\right] \\
(\mathrm{H}^{ii})_{2k-2+l,m} &= \frac{(a_1 b_2 - a_2 b_1)}{\pi}\int_{-1}^{1}\phi_k\frac{\tilde{r}_j\tilde{r}_m}{\tilde{R}^4}\,ds,
\end{aligned}
\tag{4.34}
$$

where $k=1,..,3$ and $l,m=1,..,2.$ and

$$
\tilde{r}_i = \begin{cases} a_i s + b_i - a_i & \text{when } \xi = \eta^1 \\ a_i s + b_i & \text{when } \xi = \eta^2 \\ a_i s + b_i + a_i & \text{when } \xi = \eta^3 \end{cases}
$$

$$
\mathrm{I}_k^{\mathrm{G}} = \int_0^1 2\phi_k(2t-1)|\mathrm{J}(2t-1)|\log\left(\tfrac{1}{t}\right)dt \qquad \text{and } \gamma = 1 \quad \text{when } \xi = \eta^1
$$

$$
\mathrm{I}_k^{\mathrm{G}} = \int_0^1 [\phi_k(-t)|\mathrm{J}(-t)| + \phi_k(t)|\mathrm{J}(t)|]\log\left(\tfrac{1}{t}\right)dt \qquad \text{and } \gamma = 0 \quad \text{when } \xi = \eta^2
$$

$$
\mathrm{I}_k^{\mathrm{G}} = \int_0^1 2\phi_k(1-2t)|\mathrm{J}(1-2t)|\log\left(\tfrac{1}{t}\right)dt \qquad \text{and } \gamma = 1 \quad \text{when } \xi = \eta^3.
$$

The integrals in (4.34) are not singular, therefore they will be computed using the four-point Gaussian quadrature formula. The integrals $\mathrm{I}_k^{\mathrm{G}}$ have a logarithmic singularity. The singular integrals will be computed using a Logarithmic Gaussian quadrature formula to obtain a good approximation.

5 Numerical results and discussion

In this section we show a number of results for some *simply connected* surfaces, obtained by applying the algorithm described in section 4. Note that every *simply connected* viscous fluid region Ω transforms itself into a circle when τ is going to infinity. Thus a circle must be the result of the simulations considered. Also, the fluid is assumed to be incompressible. In 2-D this means that the total surface of the moving fluid region must be constant in time. This gives us a nice criterion to monitor the accuracy of our method. In the following examples it was observed that the relative change in the total surface was less than 0.2 % when the curvature of the curves was varying moderately, and 1 % when the curvature was varying more wildly during the simulation.

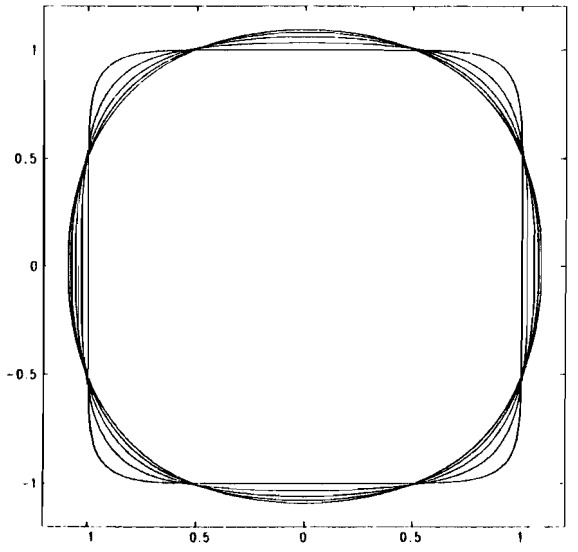

Figure 1: The transformation of an at the corners rounded off square into a circle. The various boundary curves refer to values of time τ=0.0(0.25)1.0.

EXAMPLE 1

The first class of problems to be considered is the one where the bodies have a double symmetry, which is assumed to be taken with respect to the x- and y-axis. We put the reference point $\mathbf{x}^r$ at the centre of mass: the origin. First we consider a simple geometry as shown in *figure 1*; an at the corners rounded off square, which was also considered by one of us [11]. Here the curvature κ varies only moderately, thus we do not meet the numerical problems as described in section 4.2. When $\tau = 1$, it is easy to see that the ellipse is almost a circle. The collocation points for the first quadrant, derived with both linear and quadratic elements, are in table 5.1 compared with the results derived by one of the authors [11]. During the simulation a constant timestep $\Delta\tau = 0.01$ has been taken. A closer look at the points derived from both simulation methods reveals that the differences between the same material boundary points were of the order $\Delta\tau$.

	$\tau = 0.0$		$\tau = 1.0^*$		$\tau = 1.0$ (Linear)		$\tau = 1.0$ (Quadratic)	
i	x_i	y_i	x_i	y_i	x_i	y_i	x_i	y_i
1	0.00000	1.00000	0.00000	1.09340	0.00000	1.09198	0.00000	1.09191
2	0.16690	1.00000	0.15628	1.08551	0.15683	1.08425	0.15672	1.08419
3	0.31187	0.99999	0.29053	1.06543	0.29150	1.06450	0.29130	1.06442
4	0.43814	0.99983	0.40503	1.03713	0.40640	1.03661	0.40611	1.03649
5	0.54956	0.99896	0.50317	1.00298	0.50494	1.00287	0.50456	1.00271
6	0.64666	0.99613	0.58573	0.96550	0.58786	0.96573	0.58741	0.96553
7	0.72904	0.98966	0.65318	0.92747	0.65557	0.92795	0.65509	0.92771
8	0.79517	0.97847	0.70570	0.89216	0.70814	0.89286	0.70764	0.89259
9	0.84613	0.96262	0.74576	0.86118	0.74814	0.86205	0.74768	0.86174
10	0.88350	0.94365	0.77601	0.83506	0.77825	0.83609	0.77784	0.83573
11	0.91239	0.92146	0.80129	0.81115	0.80340	0.81234	0.80304	0.81192
12	0.93751	0.89268	0.82676	0.78490	0.82866	0.78631	0.82837	0.78582
13	0.96009	0.85215	0.85602	0.75161	0.85773	0.75325	0.85749	0.75269
14	0.97809	0.79675	0.89004	0.70793	0.89155	0.70970	0.89136	0.70909
15	0.99006	0.72552	0.92794	0.65128	0.92927	0.65302	0.92909	0.65244
16	0.99648	0.63905	0.96738	0.58023	0.96850	0.58174	0.96833	0.58120
17	0.99910	0.53967	1.00500	0.49535	1.00583	0.49655	1.00569	0.49609
18	0.99986	0.42793	1.03840	0.39651	1.03889	0.39740	1.03877	0.39705
19	0.99999	0.30312	1.06557	0.28295	1.06572	0.28358	1.06562	0.28334
20	1.00000	0.16245	1.08448	0.15237	1.08438	0.15274	1.08428	0.15260
21	1.00000	0.00000	1.09195	0.00000	1.09171	0.00000	1.09161	0.00000

Table 5.1 The collocation points of the first quadrant of figure 1. These points, derived with both linear and quadratic elements are compared with the results* obtained by one of us [11]. As can be seen the deviation between the points is of order $\Delta\tau = 0.01$.

This is the best that can be expected, as mentioned in section 4.2.

EXAMPLE 2

The second example is the curve of *figure 2a*, for which the curvature is varying much more wildly during the simulation. The results obtained at different time-steps are plotted in *figure 2b*. In the boundary region near the y axis, large variations of the curvature occur. Here the collocation points will come very close to each other, and so we may lose accuracy when computing the curvature κ at those points. This problem has been solved by monitoring the distance between two successive collocation points. In our numerical algorithm, this distance is kept larger than a prescribed mimium (of order $\Delta\tau$). This example also shows that the present approach outperforms earlier work of one of the authors.

EXAMPLE 3

Thus far we have only been dealing with problems with a double symmetry. Other interesting problems in viscous sintering are ones with only one axis of symmetry. In *figure 3a* the initial shape of two cylinders of arbitrary diameters has been plotted. Recently, an analytical solution to this problem has been published by Hopper [6]. Near the contact region of both cylinders we have to deal with a large varying curvature. Again, the centre of mass (which is lying somewhere on the y axis) is taken as a reference point. The numerical results at different time-steps are shown in *figure 3b*.

EXAMPLE 4

Another example with one axis of symmetry is given in *figure 4a*. Here the cur-

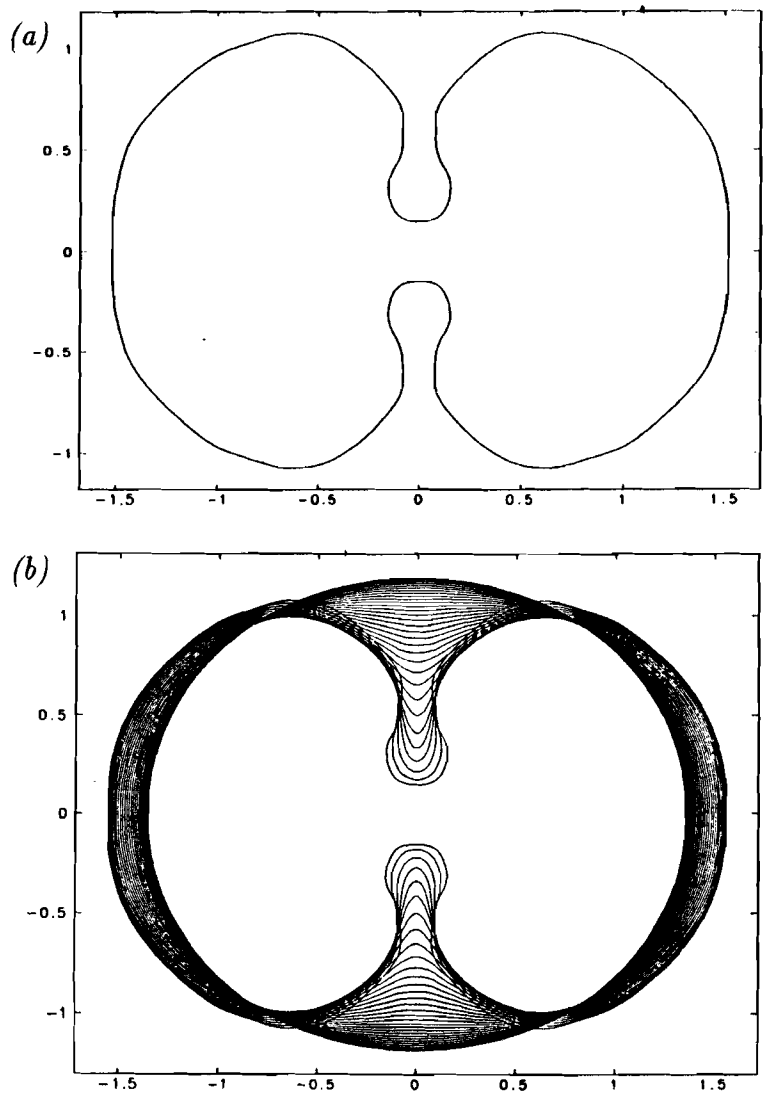

Figure 2: *(a).* The initial fluid region. *(b).* The transformation of this fluid region in time, which shows the large variation of the curvature of the outer boundary. The boundary curves refer to values of time τ=0.0(0.1)3.0.

vature is varying moderately as the time increases. The problem in this example is that we cannot take the centre of mass as a reference point, because this point does not lie in the fluid. A natural choice for the reference point seems to be the middle of the cut-off of the symmetry (y) axis in the fluid region. Because this point is going to be the midpoint, i.e. the centre of mass of the circle that will develop when the time is going to infinity. This choice gives a system of equations which appears to be a least-squares problem. This problem has been solved by a QU-decomposition method. The reason why we have to deal with a real least-square problem here is the fact that we are forcing the velocity to become equal to zero at the reference point; in reality, however, the velocity at this point is not equal to zero. The norm of the residual vector is of the order of the discretization error. The results obtained at different time steps are shown in *figure 4b.* As can be observed, first the 'mouth' of the shape opens wider,

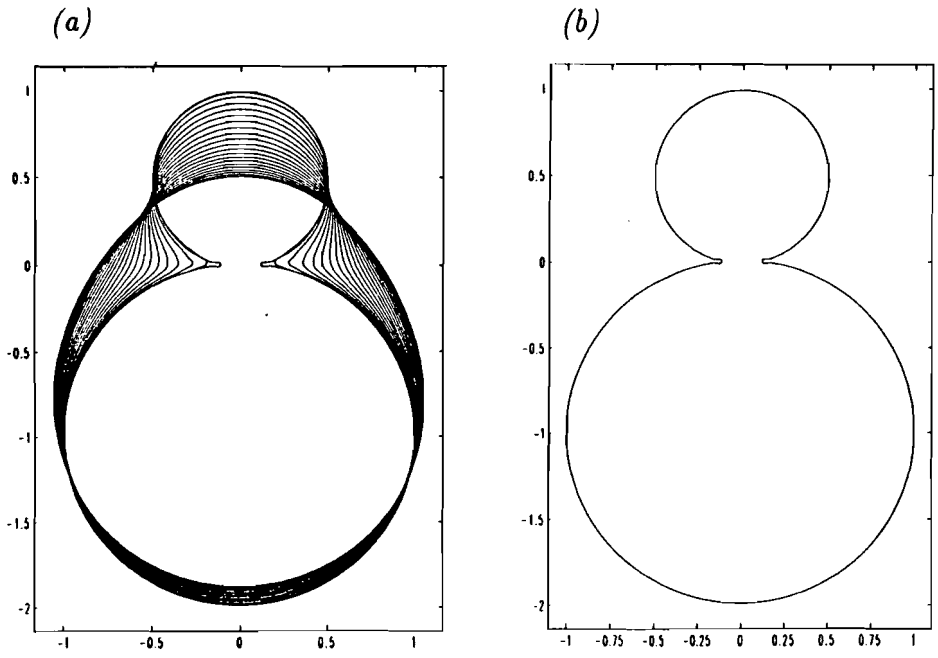

Figure 3: *(a)*. Two cylinders with different diameters. *(b)*. The transformation of these cylinders in time. The boundary curves refer to values of time τ=0.0(0.1)2.0.

and after this the fluid region develops into a circle. This phenomenon also is noticeable during the movement of example 2.
The above examples are solved using numerical algorithms which are based on linear or quadratic boundary elements. Both algorithms worked well. However, it was observed, that the algorithm based on constant elements, which are commonly used for solving this kind of problem (e.g. [3],[17]), was not stable. The physical law that the total surface of the body must be kept constant, was not satisfied during the simulation, even for a simple geometry like the ellipse of *figure 1*. The reason for this was that the system of equations as derived after discretization had only two degrees of freedom. This contradicts the results obtained in section 3.1. There it was shown that the viscous sintering problem for an arbitrary region has three degrees of freedom. Thus, somewhere in the discretization formulation, the rotation-free condition is lost. It is interesting to note that most of the other papers dealing with such problems considered symmetry situations only. In solving the problem numerically the symmetry was probably brought into the problem formulation, thus making the problem uniquely solvable.

ACKNOWLEDGMENTS

We would like to thank J. v.d. Spek [14], who did some contribution to the analysis part of this paper. This research was supported by the Technology Foundation (STW).

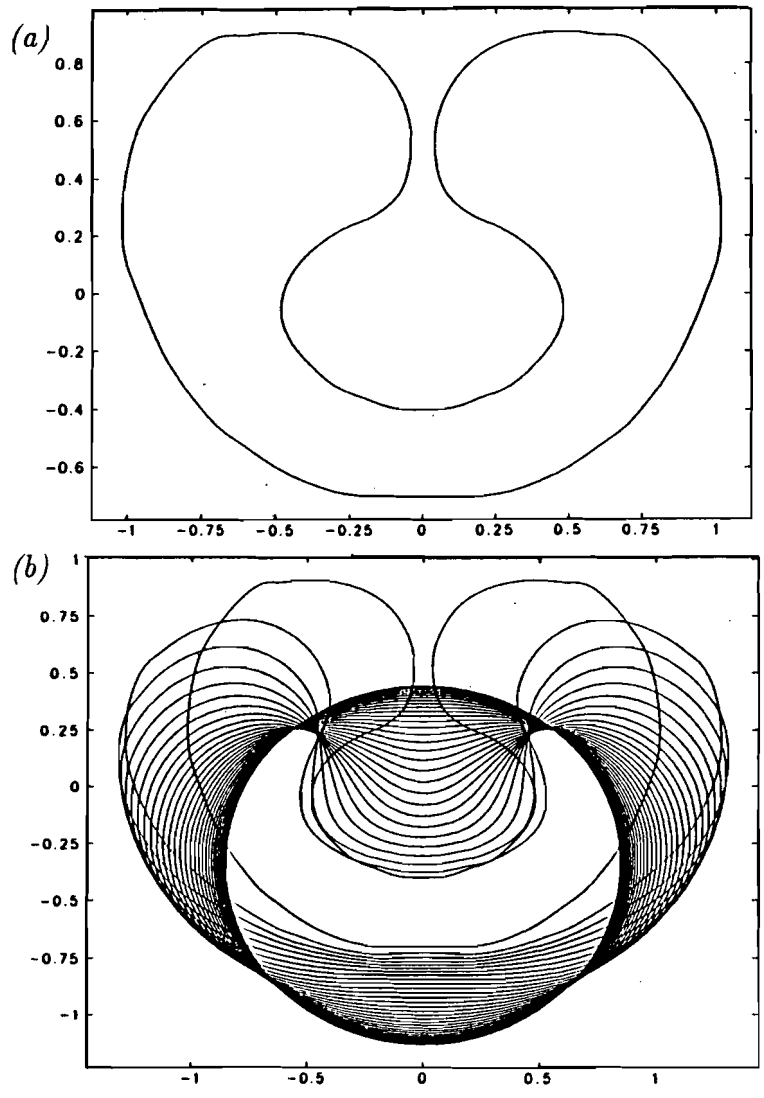

Figure 4: *(a).* Another example of a fluid with one axis of symmetry. The centre of mass of this shape lies outside the fluid region. *(b).* The transformation of these blob in time. The boundary curves refer to values of time τ=0.0(0.2)3.0.

References

[1] BREBBIA C.A. AND DOMINGUEZ J., 1989, *Boundary Elements An Introductory Course*, McGraw-Hill Book Company.

[2] BREBBIA C.A., TELLES J.C. AND WROBEL L.C., 1984, *Boundary Element Techniques. Theory and Applications in Engineering*, Springer-Verlag.

[3] CHI B.K. AND LEAL L.G., 1989, *A theoretical study of the motion of a viscous drop toward a fluid interface at low Reynolds number*, J. Fluid Mech. **201** 123-146.

[4] EXNER H.E., 1979, *Reviews on Powder Metallurgy and Physical Ceramics 1*, Freund Publishing House, Tel Aviv.

[5] HOPPER R.W., 1990, *Plane Stokes flow driven by capillarity on a free surface*, J. Fluid Mech. **213** 349-375.

[6] HOPPER R.W., 1990, *Plane Stokes flow driven by capillarity, Part 2. Coalescence of unequal cylinders*, J. Fluid Mech. (submitted).

[7] HOPPER R.W., 1990, *Plane Stokes flow driven by capillarity, Part 3. Unbounded regions*, J. Fluid Mech. (submitted).

[8] JAGOTA A. AND DAWSON P.R., 1990, *Simulation of the Viscous Sintering of Two Particles*, J. Am. Ceram. Soc. **73** 173-177.

[9] JAGOTA A. AND DAWSON P.R., 1988, *Micromechanical Modeling of Powder Compacts-I. Unit Problems for Sintering and Traction-Induced Deformation*, Acta. Metall. **36** 2551-2561.

[10] KUIKEN H.K., 1990, *Viscous sintering: the surface-tension-driven flow of a liquid form under the influence of curvature gradients at its surface*, J. Fluid Mech. **214** 503-515 .

[11] KUIKEN H.K., 1990, *Proc. Conf. on the Mathematics and the Computation of Deforming Surfaces*, Oxford University Press (to appear).

[12] LADYZHENSKAYA O.A., 1963, *The Mathematical Theory of Viscous Incompressible Flow* , Gordon and Beach.

[13] LORENTZ H.A., 1896, *Eene Algemeene Stelling omtrent de Beweging eener Vloeistof met Wrijving en eenige daaruit afgeleide Gevolgen*, Verslag Kon. Acad. v. Wetensch. Amsterdam Vol.5, 168-175.

[14] SPEK J.A.W. V.D., 1989, *Inverse Formulations for Viscous Sintering problems*, Master Thesis, Technical University Eindhoven.

[15] STROUD A.H. AND SECREST D., 1966, *Gaussian Quadrature Formulas*, Prentice Hall.

[16] ROSS J.W., MILLER W.A. AND WEATHERLY G.C., 1981, *Dynamic Computer Simulation of Viscous Flow Sintering Kinetics* J. Appl. Phys. **52** 3884-88.

[17] WEINBAUM S., GANATOS P. AND YAN Z.Y., 1990, *Numerical multipole and Boundary Integral Equation Techniques in Stokes Flow*, Annu. Rev. Fluid Mech. **22** 275-316.